Proceedings of the Fourth International Conference on Thermal Engineering: Theory and Applications January 12-14, 2009, Abu Dhabi, UAE

Spray Development of E85 and Gasoline in a Quiescent Chamber and in a Direct-Injection Spark-Ignition Engine

P.G. Aleiferis [a,] *, J. Serras-Pereira [a], Z. van Romunde [a] and J. Caine [b]

[a] *Department of Mechanical Engineering, University College London, UK*
[b] *Ford Motor Company, Dunton, UK*

Abstract

In order to investigate the impact of ethanol addition on spray formation and vaporisation from a multi-hole injector, E85 (an 85% ethanol blend with gasoline) was compared to a typical gasoline fuel (RON95) using high-speed imaging techniques in a quiescent injection chamber and in a single-cylinder direct-injection spark-ignition engine. To examine the effect of the different fuel volatilities, the injector was heated at 20 °C and 120 °C in the chamber; this was operated at 0.5 and 1.0 bar to simulate in-cylinder pressures for early injection strategies. From the results obtained fuel tip penetrations and cone angles bounding the envelope of the spray were calculated to investigate the effect of ambient conditions on spray formation. Droplet sizing was also employed in the chamber using Phase Doppler Anemometry; droplet measurements were recorded 25 mm downstream from the injector tip, along the chamber central axis. Fuel-type and temperature effects were studied in-cylinder by operating the engine at 20 °C and 90 °C head temperature at 1500 RPM. For both sets of experiments, the study was carried out for two orthogonal views, relating to the tumble and swirl planes of in-cylinder flow motion. In addition, high-speed natural light flame imaging was carried out in the engine from the swirl plane to provide information about the combustion process for both fuels, and in-cylinder pressure data were simultaneously acquired to infer burning rates. The results showed that E85 and gasoline exhibited similar spray development characteristics with small cyclic variability, although E85 had visibly thinner plumes at lower temperatures. Cone angles for E85 were typically larger than for gasoline at the same test conditions. The onset of spray collapse was similar for both fuels, with the gasoline sprays collapsing slightly more than E85 sprays at the same conditions. High-speed flame imaging and in-cylinder pressure data revealed differences in the flame structure and burning rates between the two fuels.

Keywords: Spray development, multi-hole injector, pressure chamber, direct injection spark ignition, ethanol, gasoline, flash boiling, combustion.

Nomenclature

AFR	Air-to-Fuel Ratio
AIT	After Ignition Timing
ASOI	After Start of Injection
ATDC	After intake Top Dead Centre
BDC	Bottom Dead Centre
CA	Crank Angle
DISI	Direct Injection Spark Ignition
MFB	Mass Fraction Burned
PDA	Phase Doppler Anemometry
RMS	Root Mean Square
RON	Research Octane Number
RPM	Revolutions Per Minute
SMD	Sauter Mean Diameter
SOI	Start of Injection
TDC	Top Dead Centre

* Corresponding author. Tel.: +44-20-76793862
Fax: +44-20-73880180; E-mail: p.aleiferis@ucl.ac.uk

1. Introduction

The need to reduce the dependence of the internal combustion engine on fossil fuel derived products has led to the renewed interest in the use of alcohols as a blend agent or total substitute for gasoline engines. The attractiveness comes from their comparable combustion performance and renewable credentials if derived from sustainable biological sources. There is still significant debate around which feedstock deserves the most 'renewable' label but currently sugar cane as used in Brazil is generally acknowledged to be the cheapest and best performing feedstock in terms of total green-house-gases 'well-to-wheel' emissions [1–3].

The performance of alcohols in gasoline engines has been previously documented in the literature under different studies and objectives [4–7]; however, there are very few that use current state of the art technology

fuel injection systems – namely centrally mounted multi-hole injectors with close spacing spark-plug arrangement – to understand the behaviour of different fuels under typical engine operating conditions. Moreover, many challenges remain in choosing the optimal layout of multi-hole nozzles to avoid impingement on in-cylinder surfaces or on the spark electrode while improving fuel delivery to produce the desired concentration field at ignition timing. The urgency in providing experimental data on new injection and combustion systems using current and future fuels under realistic operating conditions is thus high. It is also one of the few direct methods of validation for many fundamental fluid dynamic models and many simulation tools used in the automotive industry today.

The current work is intended as an initial study towards a comprehensive database of spray behaviour with alcohol-based fuels under realistic engine operating conditions as well as providing much needed high-speed in-cylinder spray development data which is essential for developing our knowledge of the underlying mechanisms responsible for atomisation and breakup of liquid drops in high-speed dense sprays. The results also highlight some of the obstacles facing engine design and calibration engineers in the search for better fuel economy and combustion performance using spray guided systems in Direct Injection Spark Ignition (DISI) engines. Experiments were carried out in quiescent conditions to investigate fundamental spray behaviour and quantify commonly used parameters such as spray tip penetration and spray envelope cone angles for two fuels, gasoline (RON95) and E85 (85% ethanol, 15% gasoline blend) under varying pressure and temperature conditions. Droplet sizes were also measured to investigate the effect of ethanol's different fuel properties on atomisation quality. Spray imaging results are also presented for the same injector and fuel types under similar conditions in a single-cylinder optical engine under motoring conditions. Finally in-cylinder pressure data, as well as flame images, are presented for both fuel types in order to compare the 'performance' of a high-ethanol content fuel versus standard gasoline.

2. Experimental Apparatus

Two experimental rigs were used to obtain the results presented in this paper, a single-cylinder optical engine and an optical pressure chamber. The two setups and results are discussed in separate sections below for the purpose of clarity.

2.1. Optical Pressure Chamber

A pressure chamber was used to study the spray development in a quiescent environment in order to de-couple the effects of engine intake flow on atomisation and spray break-up. An image of the pressure chamber is shown in Figure 1. The octagonal shape allows for simultaneous multi-technique characterisation, including imaging with back or side lighting and the use of off-axis techniques such as Phase Doppler Anemometry (PDA) for droplet sizing and velocity measurements. The pressure chamber facility also allows independent variation of fuel type, injector body temperature, gas pressure, and injection pressure. Further details about the pressure chamber can be found in [8].

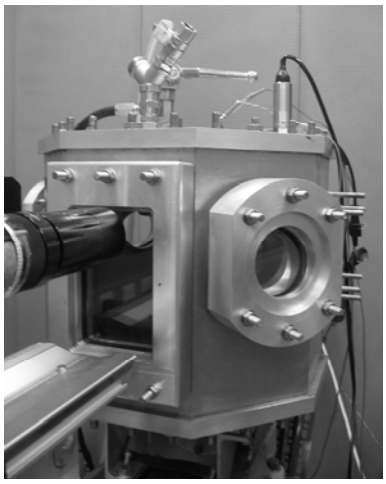

Fig. 1. Pressure chamber.

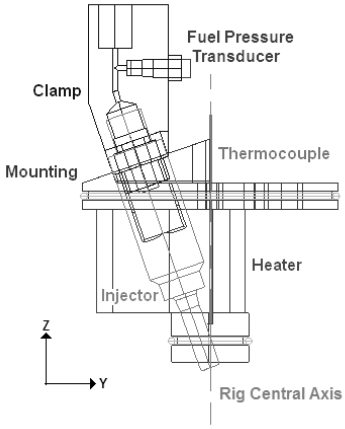

Fig. 2. Injector mounting model.

To optimise the imaging arrangement of the spray, the injector was mounted at the top of the pressure chamber at an angle of 19° (with respect to the vertical axis of the chamber). Figure 2 shows the injector mounting hardware. A 150 W band heater was used around the injector mounting for heating the injector whilst a thermocouple sensor (installed close to the injector tip) and a temperature controller allowed accurate temperature regulation. Fuel pressure was provided by a pneumatic piston ram pump which avoided pressure fluctuations in the fuel rail. The gas pressure was also monitored by a pressure transducer to ensure consistency throughout experiments.

2.2. Optical Engine

Experiments were carried out on a 4-stroke single-cylinder DISI engine. The single-cylinder engine used for this work is based on a modular Ford (US) design using a prototype DISI engine head. The engine head has a 4-valve arrangement and has similar bore and stroke geometry to that of a prototype V8 as outlined in Table 1. The engine also allows for a number of optical access configurations, namely using an extended piston arrangement with optical crown, a full quartz cylinder liner and a fixed triangular pentroof window. Further details about the engine and test cell apparatus can be found in [9]. The fuel pump used on the engine was of the same type to that used on the quiescent pressure chamber for consistency.

Figure 3 shows the engine installation with the laser and high-speed camera in place. The possible camera views using this experimental set-up are shown in Figure 4. The engine optical arrangement allows several in-cylinder views to be imaged and thus to capture the full spray development and flame growth. The view through the piston crown is useful to image both spray development and combustion as it allows all spray plumes to be seen simultaneously and also clear imaging of the first stages of flame growth from the spark plug. The view through the liner and pentroof allows imaging in the direction of the piston's motion.

Table 1. Optical Engine Specifications.

Engine Base Type	Prototype V8 Head
Cycle	4-Stroke
Cylinders	1
Valves	2 Intake, 2 Exhaust
Bore	89.0 mm
Stroke	90.3 mm
Compression Ratio	11.15:1
Valve Timings	IVO 24°, IVC 274°, EVO 476°, EVC 6°

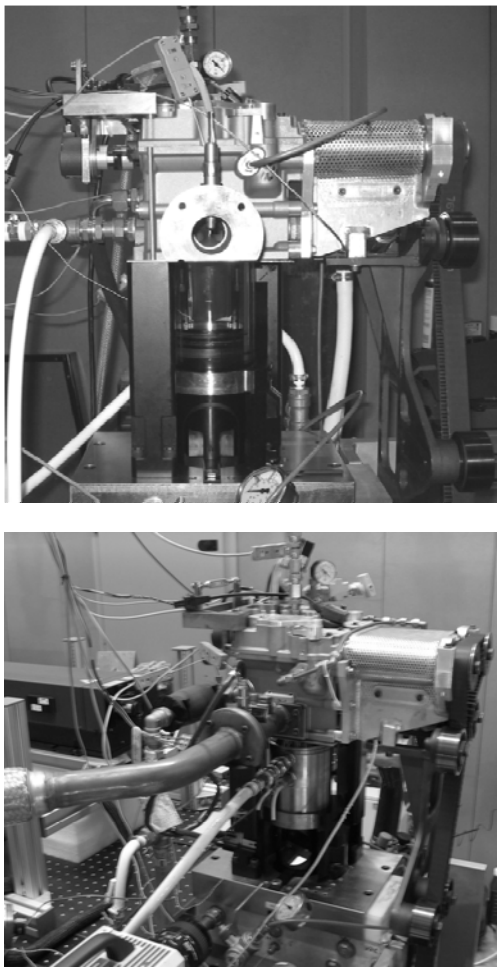

Fig. 3. Engine set-up with optical liner (top) and metal liner (bottom). The high-speed camera and laser are also visible in the lower image.

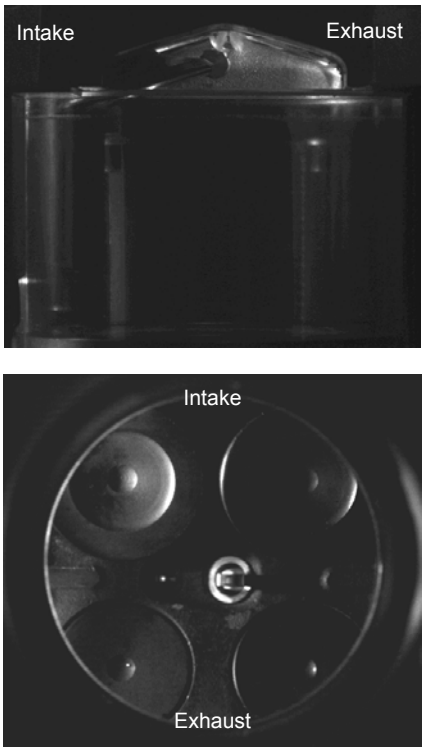

Fig. 4. Tumble (top) and swirl (bottom) imaging planes with optical engine arrangement.

2.3. Injector Geometry

A multi-hole injector producing six spray plumes in a ¾ moon pattern was used. The injector was designed for installation in the vertical position and in a close spacing arrangement with the spark plug. The six nozzle holes have different turning angles that direct fuel to different areas of the combustion chamber as shown in Figures 5 and 6 for the pressure chamber arrangement and optical engine, respectively. It should be reminded here that the injector was mounted in the pressure chamber at an angle of 19°. The illustrations in Figures 5–6 show only approximate plume directions, whilst Figure 7 shows the spray under static conditions in the engine when viewed through the piston crown at 444 μs ASOI. There is one line of symmetry in the spray pattern in the axis perpendicular to the engine's 'crossflow' axis that traverses from intake to exhaust side. Injection pressure was fixed to 150 bar.

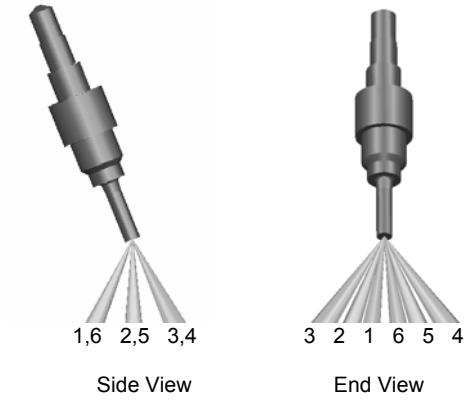

Fig. 5. Designation of the spray views used in the optical pressure chamber.

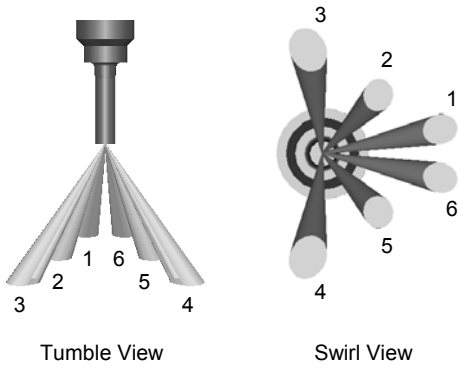

Fig. 6. Designation of the spray views used in the optical engine.

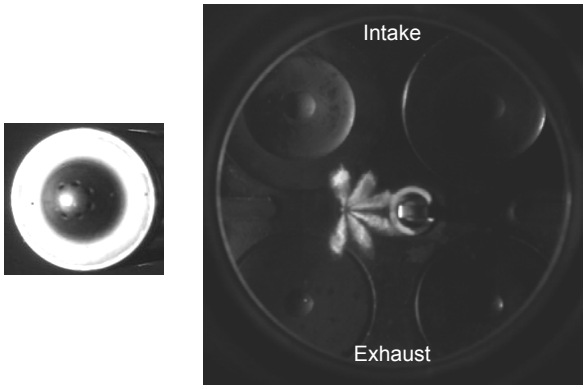

Fig. 7. Close-up picture of injector nozzle and spray image at 444 μs ASOI in static engine conditions.

2.4. Fuels

Standard commercial grade gasoline (RON95) and a commercial grade of E85 (85% ethanol mixture with 15% gasoline) were used for the present study. Both fuels were branded by the same petroleum company. Table 2 shows a number of selected properties which are relevant to the analysis of spray formation, evaporation and combustion of the fuels used; they are given for 1 bar ambient pressure. The properties of E85 were obtained from the fuel supplier specification sheet, except for the latent heat of vaporization which was estimated on the basis of values for pure ethanol (0.925 MJ/kg) and those of gasoline (0.360 MJ/kg). A relatively small set of experimental data was also acquired with pure *iso*-octane (typical single-component fuel used in engine research) to be studied as a benchmark set against the comprehensive sets of data acquired with the two multi-component fuels.

Table 2. Fuel Properties.

Fuel Properties	E85	Gasoline
Density [kg/m^3] (20 °C)	0.784	0.735–0.760
Latent Heat [MJ/kg]	0.850	0.34–0.37
Energy Density [MJ/kg] (25 °C)	28.94	42–45
Boiling Point [°C]	84.8	30–190
Reid Vapour Pressure [bar]	0.536	0.54–0.6
Research Octane Number (RON)	109.1	95
H:C, O:C	2.657, 0.411	1.86–1.92

3. Experimental Techniques

High-speed images of the sprays and flames were recorded for a series of engine cycles for both gasoline and E85. Droplet sizes were also measured by Phase Doppler Anemometry (PDA). The techniques used are described in separate sections below.

3.1. Spray Imaging

The sprays were imaged using the same experimental arrangements reported in [8] for the chamber and [9] for the engine, but the reader should note that the injection system and fuels used in the current study are different to those used in [8, 9]. Two orthogonal views were used on both rigs, termed 'Side View' and 'End View' in the pressure chamber (as shown in Figure 5), and 'Piston Crown View' or 'Swirl View' and 'Pentroof Window View' or 'Tumble View' in the engine (as shown in Figure 6), the latter view being equivalent to the 'End View' in the chamber. A Photron APX-RS high-speed camera was used with a frame rate set to 9 kHz, *i.e.* the equivalent of one image per degree Crank Angle (°CA) degree for an engine running at 1500 RPM. The spatial resolution was 640×480 pixels at this frame rate and the shutter was set to 1 μs in the chamber and 4 μs in the engine. This resolution was used for all spray imaging done in the pressure chamber and for all images acquired through the piston crown view (swirl view) in the engine. However, for the spray imaging on the tumble plane (pentroof window view), the spatial resolution was adjusted to 512×1024 to allow the full spray development to be captured in the axial direction (*i.e.* in the direction of piston motion) and, thus, the frame rate was decreased to 5 kHz. Spray illumination was performed in the pressure chamber by backlighting using a Multiblitz Variolite 500 photographic flash-lamp. As a result of this arrangement, each imaged jet in the pressure chamber is the superposition of two liquid jets for the side view (Figure 5). The image produced is a shadowgraph of the spray and as a result only the liquid-phase is visualized with this technique. Similarly, a Mie-scattering technique employed in the engine allowed only the liquid phase to be investigated. This was done by global spray illumination with a high-repetition rate Nd:YLF laser (New Wave Pegasus), firing synchronised to the same frequency of the high-speed camera (9 kHz or 5 kHz). For the spray images acquired through the piston crown (swirl view), illumination was provided from the side (*i.e.* through the pentroof window), whilst for the spray images acquired through the pentroof window (tumble view), illumination was provided from below (*i.e.* through the piston crown).

The raw test images from the pressure chamber were checked for suitability of lighting and triggering to reduce the analyzed batch to 100 runs and 1 background set. The background image was removed from the spray images to account for differences in lighting over the run. Each corrected image was then thresholded at a value based on the mean of background pixels to leave a binary image. Due to the different angles at which each plume pair emerges from the nozzle tip, the image was then rotated to align each plume pair with the vertical axis and each plume was then 'scanned' to find the plume tip. The distance from the plume tip to the nozzle was scaled to calculate a plume pair length. A similar procedure was used to

obtain the overall spray envelope cone angle. In the engine 100 consecutive motoring cycles with injection were imaged and then averaged to find the mean spray envelope; the standard deviation (or RMS) image was also calculated to illustrate areas of 'variability' within the spray.

3.2. Flame Imaging

Flame images were acquired at a frame rate of 9 kHz in the swirl plane *i.e.* 1º CA between frames at 1500 RPM. The combustion process was visualised by imaging the natural light flame chemiluminescence on a cycle-by-cycle basis for 100 consecutive cycles. In-cylinder pressure data were recorded simultaneously. This allowed the imaging data to be compared to burning rates derived from the pressure data to extract information about flame growth characteristics and sources of cycle to cycle variations.

3.3. Droplet Sizing

Droplet sizing of the spray was carried out using a TSI Phase Doppler Anemometry system consisting of a Coherent Innova 70C Argon-Ion laser coupled to a TSI beam splitter and Bragg cell. Both the transmitter and receiver had an optical focal length of 250 mm. The forward scattering angle was set to 40°. Laser power was set to 0.5 W to avoid over saturation. Due to the plume liquid density being quite high near the nozzle, droplet measurements were recorded 25 mm downstream from the injector tip, along the chamber central axis. Measurements were taken in the centre of plume 2, which is the central plume nearest the camera as the spray is seen from the side (Figure 5). The measurement system was moved in the x-axis to ensure measurements were taken in the centre of the plume for all conditions. Droplet size measurements were taken over 200 injections for all conditions.

4. Experimental Conditions

The experimental conditions were selected to represent low-load or full-load engine operation with injection timings early in the intake stroke to promote homogeneous mixture formation, as described below.

4.1. Pressure Chamber Test Conditions

To mimic the conditions surrounding the injector body when mounted in an engine, the injector body was heated to temperatures of 20 and 120 °C. The assumption was made that given a settling time of at least 1/2 hour and an injection frequency of less than 1 Hz, the fuel inside the injector would reach similar temperatures to that of the surrounding injector body. Part-load and early injection engine strategies were replicated by inducing a vacuum in the pressure chamber. For simulation of early injection homogenous charge operation, a gas pressure of 0.5 bar (absolute) was created in the chamber.

4.2. Engine Operating Conditions

The baseline operating conditions are given in Table 3. The engine was motored at part load (0.5 bar intake pressure) and fired at the same load continuously, *i.e.* with no skip-firing. A piezo-resistive absolute pressure transducer was installed in the inlet plenum to set the engine load by adjusting the throttle as necessary. The engine was run with stoichiometric Air-to-Fuel Ratio (AFR), *i.e.* equivalence ratio Φ=1 (or air excess ratio λ=1), for all the tests presented in the current paper. An AFR meter was used in the exhaust to measure oxygen content and this was used for setting the correct fuelling at the required engine operating point. The influence of temperature on spray development and combustion was observed by changing the engine coolant temperature from 20 °C to 90 °C.

The Injection timing was set for homogeneous mixture preparation mode, *i.e.* early in the intake stroke, with Start of Injection (SOI) set to 80° CA ATDC, in order to maximize the time available for evaporation before ignition. This decision was balanced by the need to avoid excessive liquid impingement on in-cylinder surfaces, particularly on the piston crown which would affect the imaging arrangement by fouling the windows. Spray interactions with the intake valves were also explored by using injection timings either side of 80° CA ATDC (namely 60° CA and 120° CA ATDC). Depending on the valve timing used, significant interactions with the intake valves can take place which alter the targeting of fuel by the injector and subsequently affect the global in-cylinder fuel distribution. Two injection durations were used in the tests carried out. The smallest (0.8 ms fuel pulse duration) was employed to keep engine surfaces relatively dry and improve image quality for purposes of spray image processing; the second pulsewidth was actually the correct duration for stoichiometric firing operation at 1500 RPM at part-load for each fuel (1.25 ms for gasoline and 1.6 ms for E85).

For the firing tests, ignition timing was fixed to 35° CA before compression TDC, *i.e.* at 325° CA ATDC. 100 consecutive cycles of in-cylinder pressure data were acquired after the engine was fired and had been allowed to stabilise for 20–30 s. Synchronization of various control triggers was done with an AVL Engine Timing Unit. In-cylinder pressure data and processing to infer performance statistics for each cycle such as Mass Fraction Burned (MFB) was done using LABVIEW and MATLAB based software [9].

Table 3. Engine Operating Conditions.

Engine Speed	1500 RPM
Intake Air Pressure	0.5 bar
Injection Pressure	150 bar
Engine-Coolant Temperature	20 °C and 90 °C
Ignition Timing	325° CA ATDC
Equivalence Ratio	Φ=1

5. Results and Discussion

The results obtained are presented in separate sections for the pressure chamber and the optical engine, as follows. This is done for better clarity in the discussion.

5.1. Pressure Chamber

Typical spray images for E85 and gasoline at 777 µs ASOI for different conditions are presented in Figure 8 for the side view and Figure 9 for the end view. *Iso*-octane was only imaged through the side view as it did not form an integral part of the work, but it was included as a 'model' fuel for relative comparisons only.

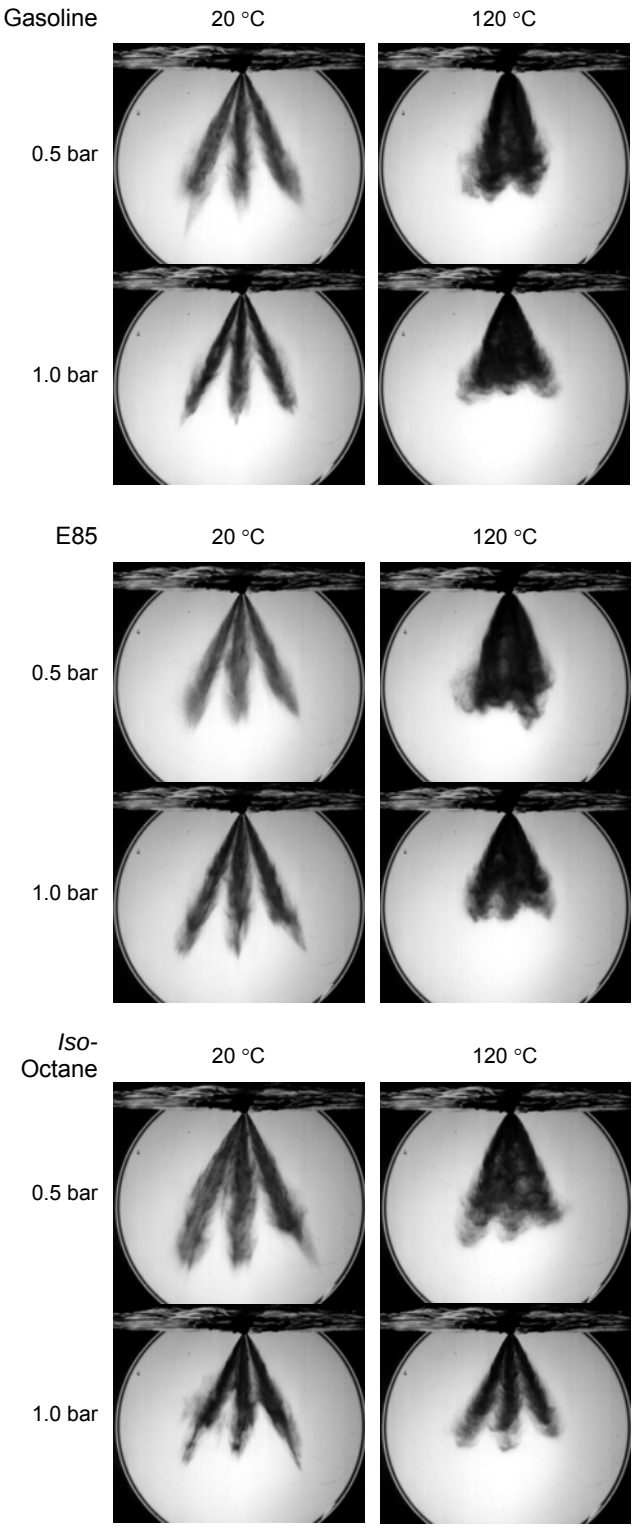

Fig. 8. Fuel comparison of spray development inside the pressure chamber for the side view.

In general, at low injector temperatures *i.e.* 20 °C, gasoline and E85 sprays showed similar macroscopic behaviour at both 0.5 bar and 1.0 bar gas pressures. However, there are noticeable differences as far as the break-up behaviour of individual plumes is concerned. Specifically, at 1.0 bar, the individual spray plumes of E85 were noticeably thinner and more compact, appearing not to break up as easily as those of gasoline; this is particularly clear in the end view shown in Figure 9. Spray development movies showed that both *iso*-octane and gasoline sprays were strongly affected by air entrainment into the spray leading to noticeably higher levels of spray dispersion around the plumes as a result of more efficient atomisation. The leading edge of the spray plumes for E85 appear much more 'needle-like' (particularly at 1.0 bar gas pressure) and produced the classical single-hole pressure-jet spray pattern typically referred to as a 'fishbone' structure; this is represented by a thin core and a trail of atomised fuel droplets on either side which are stripped from the plume as a result of drag and gradual break-up. Similar observations using other types of multi-hole injectors and fuels have been reported in [10, 11]. The direct effect of these compact E85 spray plumes is increased penetration in comparison to the spray plumes produced by gasoline as discussed later in this paper.

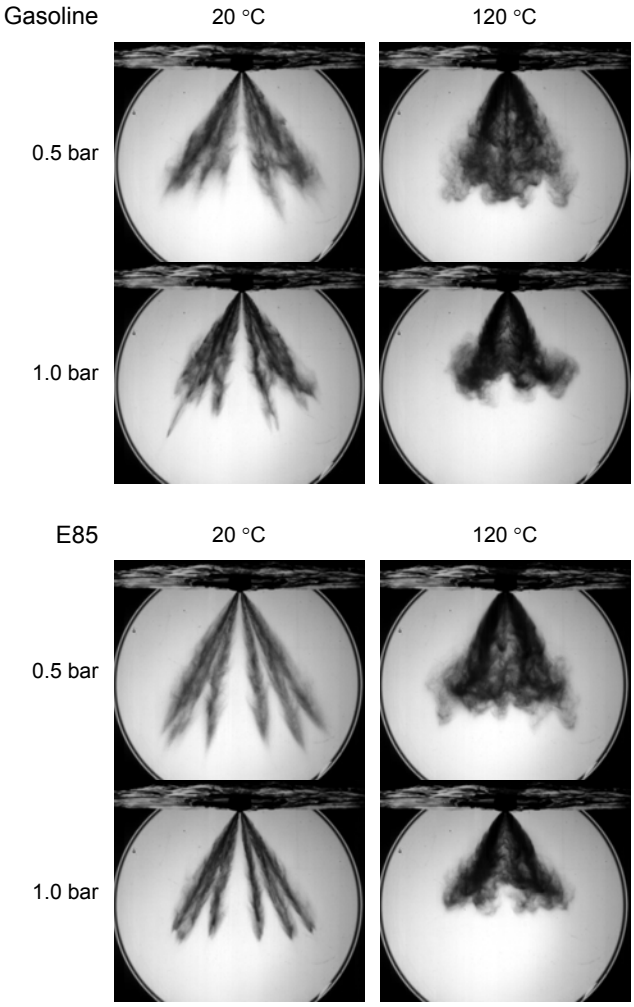

Fig. 9. Fuel comparison of spray development inside the pressure chamber for the end view.

At high temperatures, 120 °C, and at both 0.5 bar and 1.0 bar gas pressures, the gasoline spray was seen to collapse to a greater extent than the E85. Specifically, at 0.5 bar gas pressure, the gasoline plumes merged into a 'single' plume below the injector and formed a 'collapsed' spray, showing a clearly lower width at the waist of the spray than for E85 and this is reflected in the lower calculated spray cone angles presented later in this paper.

At 1.0 bar both the gasoline and the E85 sprays have also undergone significant collapse at 120 °C, although the E85 is again less affected and the spray cone angle is greater as a result of the remaining spray directionality. Although at 20 °C the sprays of gasoline, E85 and *iso*-octane are all similar in the side view (Figure 8), the extent of spray collapse for *iso*-octane is much less at 120 °C and the three individual plume pairs can still be clearly identified, particularly at 1.0 bar gas pressure as a result of *iso*-octane's higher boiling point (99 °C).

The greater sensitivity of gasoline to collapse is believed to occur as a result of the different distillation curves of the two fuels. Pure ethanol has a boiling point of 78.5 °C at 1 bar. Due to its high ethanol content, E85 has a boiling point of ~85 °C with a distillation curve that is nearly vertical, whereas gasoline's distillation curve has a gradually increasing slope with an overall boiling point of ~77 °C (mid of the distillation curve). As gasoline is a multi-component fuel it contains a portion of chemical components which boil at significantly lower temperatures, *e.g.* pentane boils at 36 °C at 1 bar ambient pressure and the higher degree of superheat experienced by some these chemical constituents of the multi-component blend are believed to be responsible for the 'flashing' phenomena observed [8]. The exact mechanism behind 'flash boiling' and 'spray collapse' is also believed to stem from the coupling with in-nozzle phenomena, like cavitation which results from the pressure drop experienced by the fluid as it enters the nozzle passage [12]. This complex mechanism is currently under study using real-size optical nozzles and the findings will be reported in a future publication.

The results of image processing are shown in Figures 10–12 for gasoline and E85 at each test condition. The plume tip penetration is presented for the left plume pair (plumes 1/6) due to the differing absolute lengths of the plume pairs. However, all plume pairs illustrate the same penetration trends in relation to the conditions. Comparisons between the two fuels for plume tip penetrations at 0.5 bar and 1.0 bar gas pressure are made in Figures 10 and 11, respectively, for 20 °C and 120 °C. Overall spray cone angles are shown in Figure 12.

It can be observed that for gasoline at 20 °C there is an average reduction in spray tip penetration of ~2 mm with increased gas pressure (from 0.5 to 1.0 bar). The spray tip penetration of E85 was less sensitive to changes in gas pressure but was always higher than gasoline at 20 °C by ~4 mm. The increase in temperature has a much greater effect on spray tip penetration in general. At both 0.5 bar and 1.0 bar gas pressure the penetrations are markedly reduced for both fuels. For 0.5 bar gas pressure, the average penetration for gasoline at 120 °C drops by ~20% compared to that at 20 °C; for E85 the reduction is ~30%, illustrating the effect of greater collapse and downward spray momentum for gasoline. The effect of higher temperature on the two fuels at 1.0 bar is very similar, with both experiencing a 38% decrease in penetrations as a result of similar levels of evaporation and degree of spray collapse.

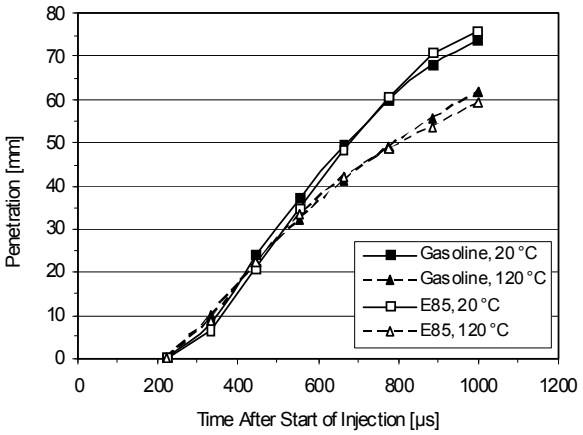

Fig. 10. Spray Plume penetration in pressure chamber for 0.5 bar gas pressure.

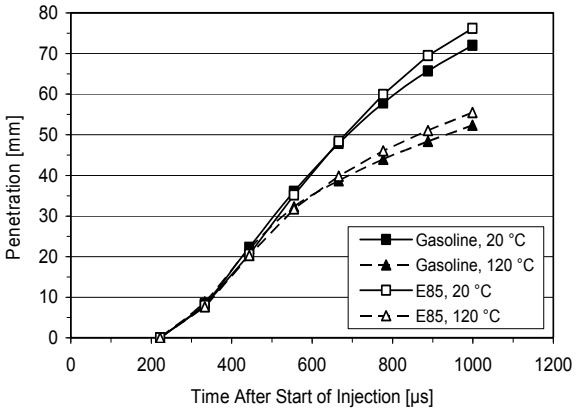

Fig. 11. Spray Plume penetration in pressure chamber for 1.0 bar gas pressure.

An interesting observation with regards to spray tip penetration is that E85 always appears to start with a lower penetration than gasoline immediately after the arrival of fuel at the injector tip. This phenomenon was also observed in the spray images acquired from the optical engine (as shown later), as well as observed in another study using pure ethanol and a similar multi-hole injector with a different nozzle arrangement [12]. The similar observations indicate that the different liquid properties of ethanol somehow affect the rate at which the fuel travels inside the injector, or perhaps affects the speed at which the needle opens and closes, albeit by only a few tens of microseconds. The higher viscosity of ethanol compared to gasoline could be potentially responsible, particularly since the effect is less accentuated at higher temperatures where viscosity is substantially reduced.

The combined spray envelope angle, as measured between 2 and 22 mm from the injector tip by processing the side view spray images, demonstrates

the level of convergence of the spray plumes. This is shown for 0.5 bar gas pressure in Figure 12. At 20 °C, the spray angles for both fuels are essentially the same, ~59°, but decreased under spray collapse conditions to ~48° for gasoline and 52° for E85 at 120 °C, reductions of nearly 20% for gasoline and 12% for E85.

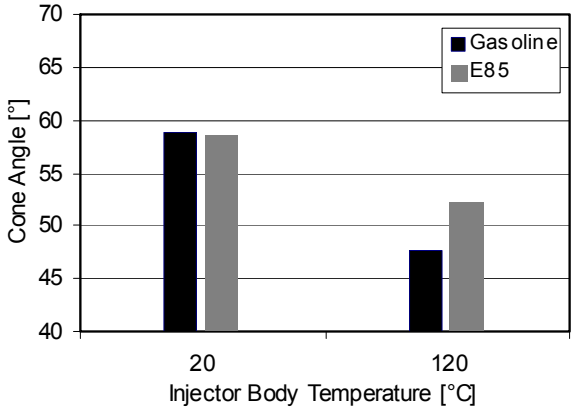

Fig. 12. Average spray angles from pressure chamber at 0.5 bar gas pressure.

In order to investigate further the link between the spray development and atomisation, droplet sizing was carried out in the chamber for a range of gas pressures and injector temperatures. Figure 13 shows the values of Sauter Mean Diameter (SMD, $D_{3,2}$) measured 25 mm below the injector tip for plume 2. This showed that for 0.5 bar gas pressure, droplet sizes decreased with an increase in injector temperature, ranging from ~21 to 9 µm for gasoline and ~28 to 10 µm for E85. In fact, E85 always showed larger droplets than gasoline by ~25%, with the highest differences found at the low temperature and low pressure conditions. This may stem from E85's higher latent heat of vaporisation, cooling the gas temperature and reducing the droplet evaporation rates. At higher temperatures, with high levels of superheat for both fuels, the differences became smaller, only ~15% higher droplet sizes for E85 relative to gasoline.

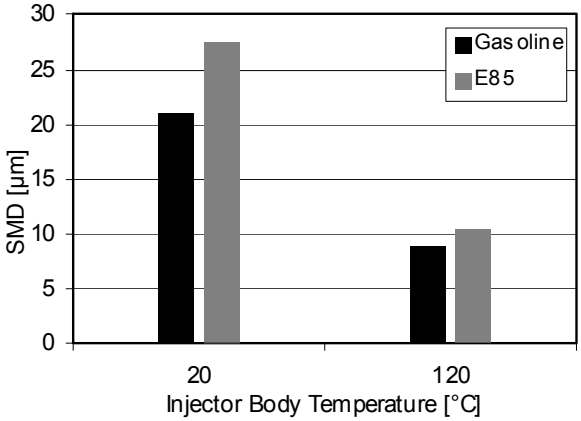

Fig. 13. Spray SMD from pressure chamber at 0.5 bar gas pressure.

Only a few of other studies have been found to report droplet size data from multi-hole injectors under similar conditions, *e.g.* [12], and only one using E85 [13]. The general observations in terms of spray behaviour and droplet sizes between gasoline and E85 were consistent with those found here however the different geometries of the injectors and the varying operating conditions used make specific comparisons difficult. Other studies using pressure-swirl injectors [7, 14] have also reported similar behaviour between sprays of gasoline and those of E85 under high-temperature low-pressure conditions, with spray collapse also reported at high engine cooling temperatures.

5.2. Optical Engine

Two images of a spray, one in the chamber and one in the engine at static conditions are shown in Figure 14. To improve the complete visualisation of such a complex spray, the injector in the chamber was mounted at 19° to the vertical. Thus, what appears to be difference in spray tip penetrations for the centre plumes compared to the engine are in fact artefacts of the imaging arrangement and injector mounting angle. Any comments will therefore relate to structural macroscopic differences between the chamber and the engine in terms of spray formation and break-up, as well as overall observations of the spray sensitivity to fuel temperature and ambient pressure.

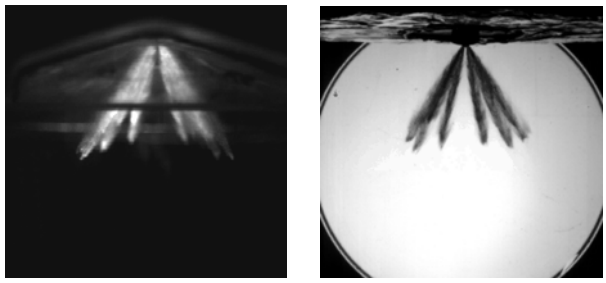

Fig. 14. E85 spray in the engine at 600 µs ASOI (left) and in the pressure chamber at 555 µs ASOI (right) at 20 °C, 1.0 bar.

Sprays from representative cycles are shown in Figure 15 for the swirl plane using three different injection timings, initially investigated with gasoline under motoring conditions. It became clear that with the current valve timing set-up, injection timings starting later than ~80° CA ATDC did not lead to satisfactory fuel distribution and mixing as a result of significant interactions with the opening intake valves. The image of Figure 15(c) shows the impinging spray plumes on one of the intake valves in particular, destroying the intended directionality provided by design of the nozzle holes. For earlier injection timings, valve interactions do not occur nearly as much (dictated by the length of the injection pulse); however, the higher piston position does have negative implications in the form of greater direct impingement on the piston surface which result in pool fires if the fuel films have not evaporated fully by ignition timing. Although at 90 °C engine coolant temperature this was not found to be a significant issue, at 20 °C the locations of impinging sprays were clearly marked out on the piston window and visible at the end of a test run; these also showed brown marks around the impact location after firing, supporting the hypothesis of potential pool fires when using such strategies at low temperature conditions. As a result of these findings, together with confirmation of superior combustion stability with start of injection timing set to 80° CA ATDC, this injection timing was finally used for

all subsequent tests. Then, sprays were studied for part-load operation (0.5 bar intake pressure) and full load (1.0 bar intake pressure) at 7° CA ASOI (*i.e.* 87° CA ATDC); however, data was collected in the ranges 80°–140° CA ATDC (intake stroke) in the swirl plane and 80°–152° CA ATDC in the tumble plane.

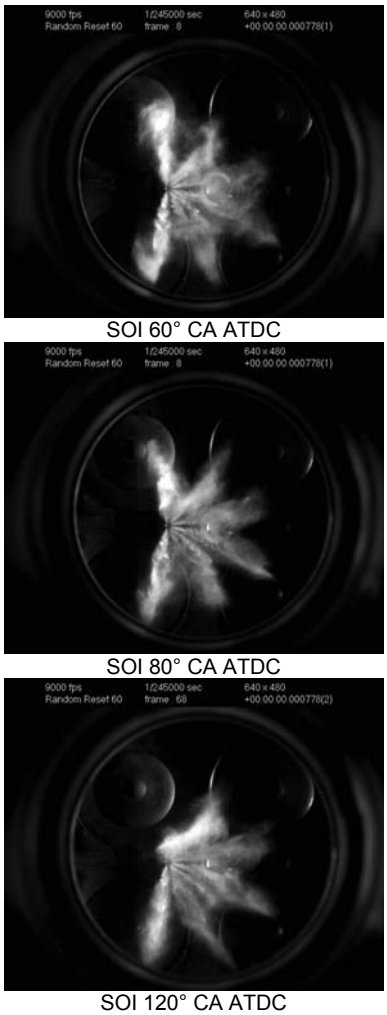

Fig. 15. Gasoline spray at 7° CA ASOI for different injection timings with 0.5 bar intake pressure.

5.2.1. Swirl Plane Spray Imaging

Figure 16 shows representative sprays in the swirl plane for gasoline and E85 at 20 °C and 90 °C engine coolant temperatures under part-load operation. It is generally observed that the E85 spray was visually very similar to that of gasoline at 20 °C and 90 °C. The average and RMS spray images shown in Figure 17 are more helpful though in describing the actual spray behaviour. It is clear from these that at 20 °C the E85 spray has better defined plumes and the areas between the plumes are on average free from the levels of atomised spray seen for gasoline, illustrated by the blurred outline of the plumes. In fact, there is definition between the plumes for E85 even in the near nozzle region which shows that there is certainly a different level of atomisation taking place immediately outside the nozzle, *i.e.* levels of air entrainment and thereby the break-up are probably different from that of gasoline. The RMS image also shows the same trends in terms of spray geometry but indicates that shot-to-shot variability of E85 on a cycle by cycle basis is more comparable to gasoline, even though the latter shows marginally higher plume variability envelope, probably as a result of faster break-up and a greater sensitivity to cyclic variations in the bulk flow-field.

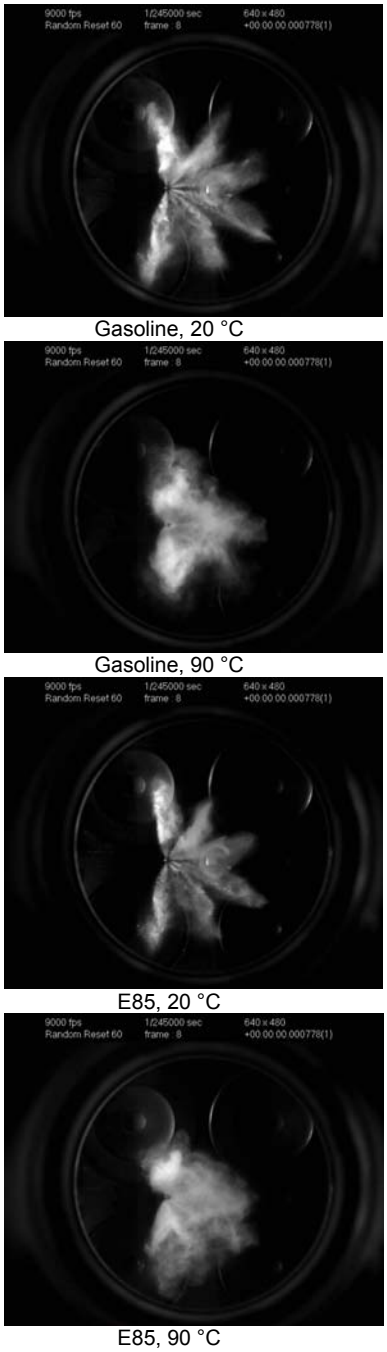

Fig. 16. Swirl plane sprays for gasoline and E85 at 7° CA ASOI with 0.5 bar intake pressure.

At 90 °C the gasoline spray is seen to ‘collapse’ to the same degree observed in the pressure chamber at 120 °C. The partial loss of directionality for all plumes is shown by the concentration of the spray in the centre of the piston crown as the spray momentum becomes biased in the vertical component. Similar behaviour was observed for both E85 and gasoline at these conditions although E85 collapsed to a slightly lesser extent than gasoline. This was visible immediately in the first

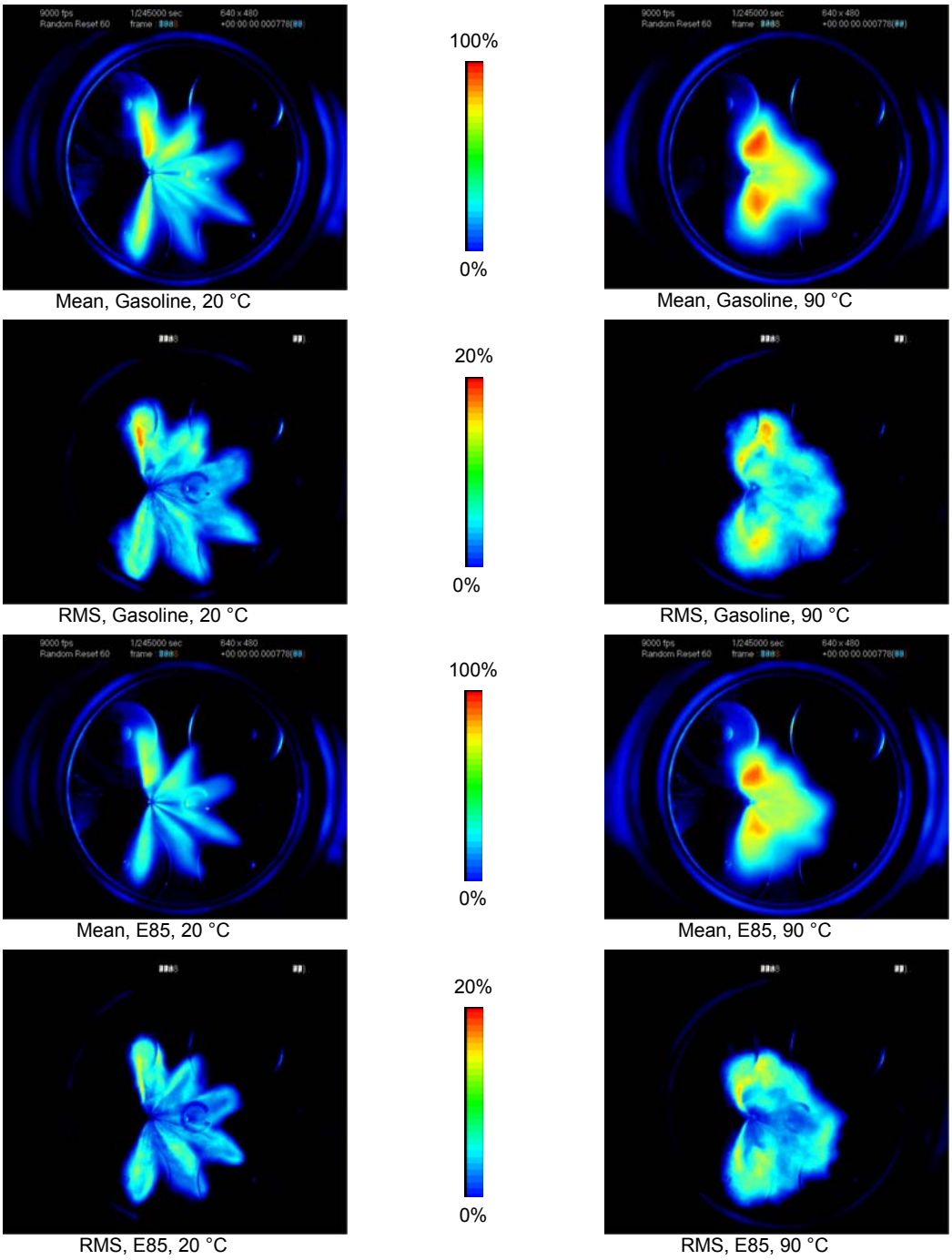

Fig. 17. 100-cycle mean and RMS sprays on the swirl plane at 7° CA ASOI with 0.5 bar intake pressure.

imaging frame of each spray development (*i.e.* in the frame where fuel was seen exiting the nozzle for the first time during the injection process; typically about 2–3° CA ASOI). In fact, gasoline was already clearly flash-boiling, in contrast to E85 where the six individual plumes were still identifiable. Compared to the pressure chamber, the trends from this engine plane are consistent, although it is difficult to make comments on spray angles and penetration from this view. The following section will address more direct comparisons with the pressure chamber since the engine tumble plane view is directly comparable to the chamber's end view (apart from the differences in perspective that result from the 19° injector inclination in the chamber).

5.2.2. Tumble Plane Spray Imaging

Since the tumble plane provides imaging data that is more easily interpreted and comparable to the pressure chamber's end view, the sprays are shown for both part-load and full-load conditions in Figure 18. The first observation during the injection period was the occurrence of clear liquid impingement on the piston crown for both fuels and at both cold and hot engine conditions, particularly at 0.5 bar gas pressure. The E85 performs poorly in this respect because of the longer pulse width required (28% longer compared to gasoline for the conditions used) as a result of its lower

stoichiometric AFR (note that the stoichiometric AFR ratio for pure ethanol is 9, whilst for gasoline is typically 14.7). This also affects the interactions with the intake valves as shown previously in Figure 15 and the effect of the cylinder walls 'pushing' the spray to the centre of the cylinder towards the end of injection. The effect of longer pulses has also been associated with greater HC emissions with ethanol, especially at full-load conditions and low engine speeds [15]. The effect of in-cylinder flow on spray development and break-up should be noted by comparing with the static engine spray in Figure 14. Different levels and locations of impingement on the piston crown were seen for 20 °C and 90 °C with smaller yet targeted impingement occurring at 20 °C and more disperse mixing/flow-controlled impingement at 90 °C as the collapsed spray cloud is drawn together towards the centre of the chamber. The magnitude of spray collapse at 90 °C was similar for both fuels but marginally higher for gasoline. The level of spray break-up was also clearly greater for gasoline and this is illustrated by the lack of a coherent structure in the spray compared to E85, where the main plume pair can still be identified; the results are thus consistent with observations from the pressure chamber. At full load (1.0 bar intake pressure), the images at 20 °C are remarkably similar to those at part load, although there is greater spray dispersion around the plumes due to the greater drag forces. At 90 °C, however, there is a noticeable but similar reduction in the spray tip penetration for both fuels. Spray collapse does not really take place, and the directionality is maintained to a large degree. There are significant improvements in atomisation and break-up which result in faster evaporation; the removal of the leading edge by stronger in-cylinder flow is probably another factor in the reduction in tip penetration observed.

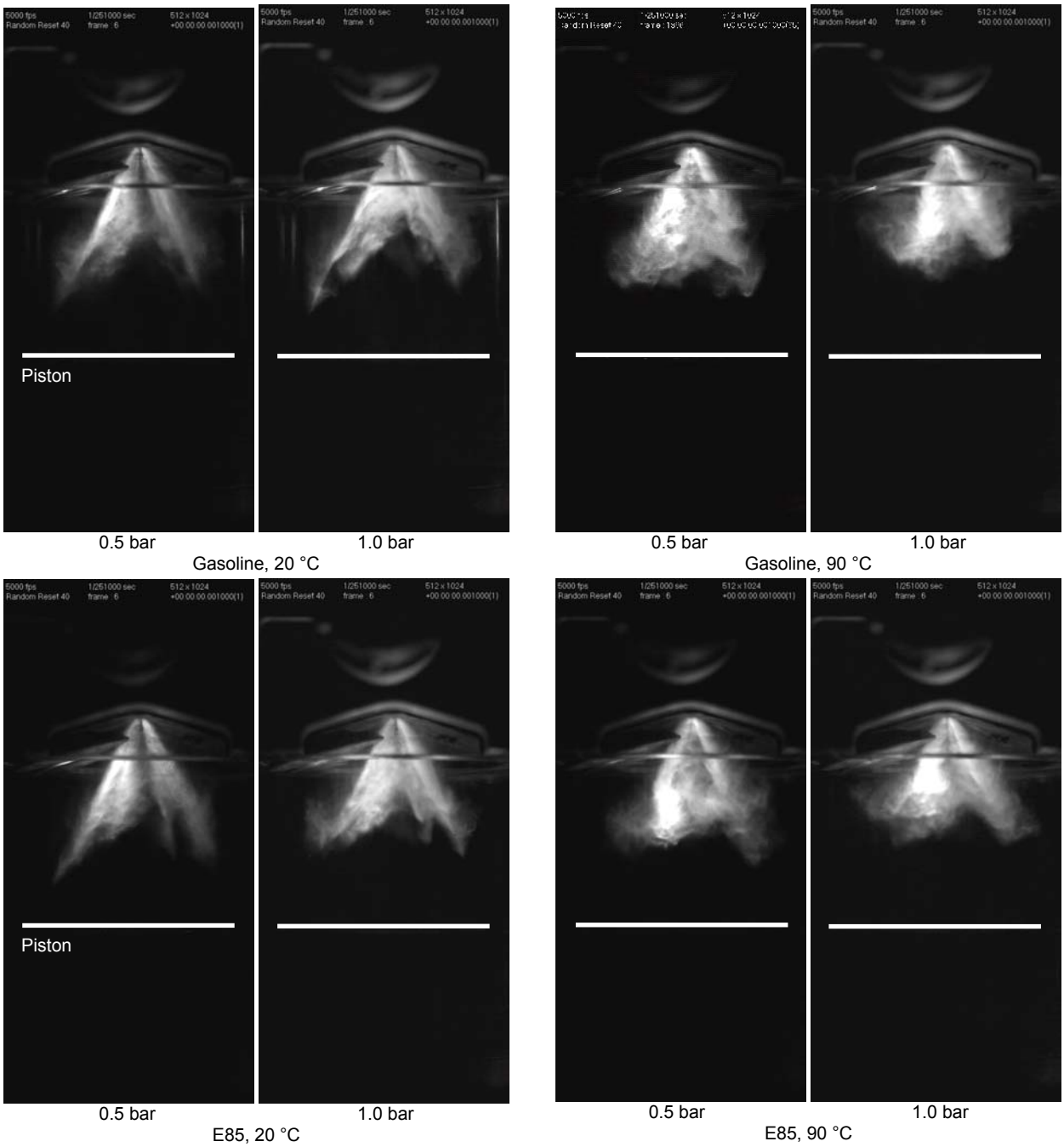

Fig. 18. Tumble plane sprays for gasoline and E85 at 9° CA ASOI.

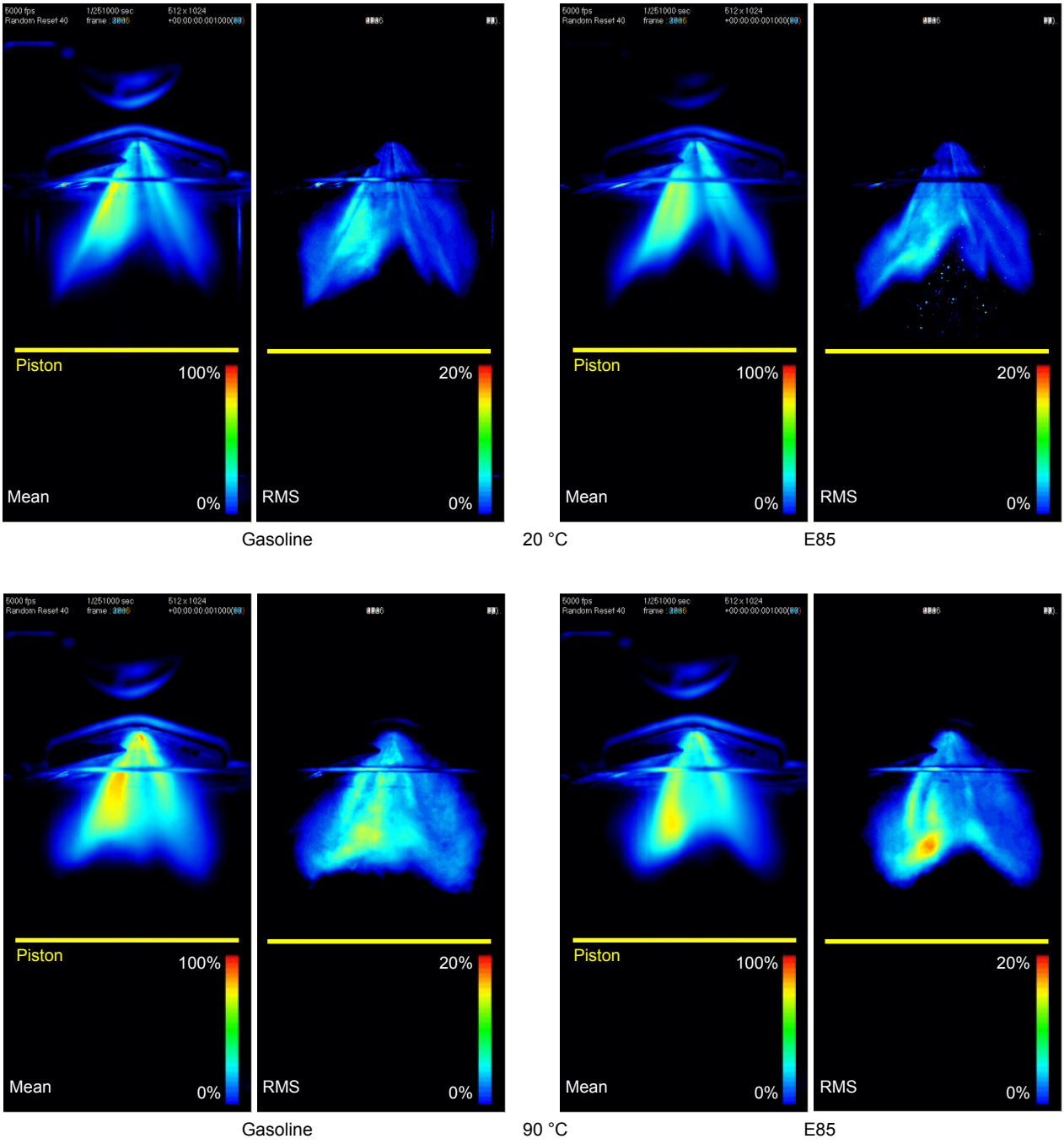

Fig. 19. 100-cycle mean and RMS sprays on the tumble plane at 9° CA ASOI with 0.5 bar intake pressure.

In Figure 19 the average and RMS images are again used to gauge the shot-to-shot variability of the macroscopic spray development at part load. At 20 °C the mean images of E85 and gasoline show very few visual differences between the sprays. However, the RMS images are more useful in interpreting the differences in atomisation quality. For example, it can be seen that E85 has a noticeable number of RMS droplets in the image above the piston. These droplets are not artefacts of image processing; they indicate that in some cycles there was at least one or more droplets or group of droplets large enough to be imaged below the main spray and that for gasoline no such droplets existed, *i.e.* the atomisation quality of E85 at 20 °C is inferior to gasoline, with such droplets being too large to be completely entrained in the flow and probably impinging on the piston crown. The gasoline spray also shows more spray swelling under the low pressure region of the intake valve, indicative of better atomisation and break-up. The same trends are seen at 90 °C although droplets are no longer shown in the RMS image for E85. The RMS image for gasoline shows a wider footprint as a result of greater collapse whereas for E85 some directionality remains.

5.2.3. Swirl Plane Flame Imaging

Flame imaging was carried out to investigate the differences between E85 and gasoline in terms of flame growth rate and flame motion. The engine was operated at part load (0.5 bar intake pressure) with the same injection timing used for spray analysis (SOI 80° CA ATDC) and a spark advance of 35° CA for both fuels. Both 20 °C and 90 °C engine coolant temperatures were investigated. Images of typical flames are presented for the swirl plane in Figures 20 and 21.

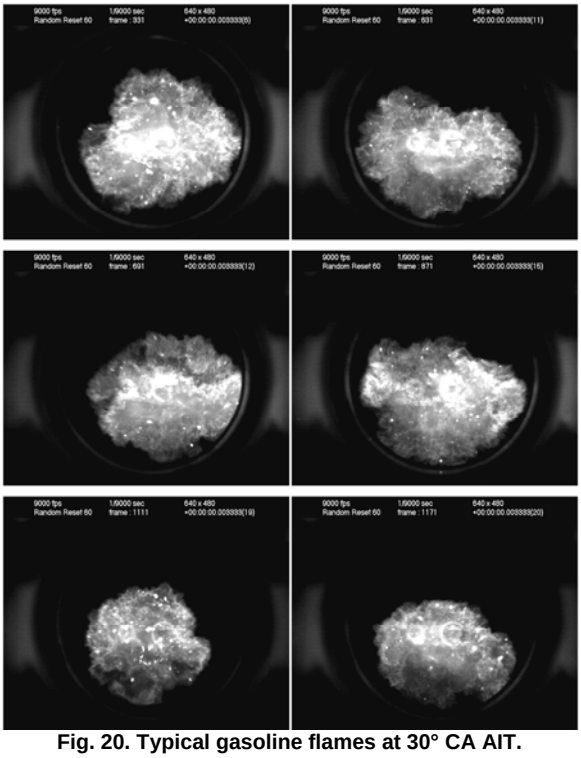

Fig. 20. Typical gasoline flames at 30° CA AIT.

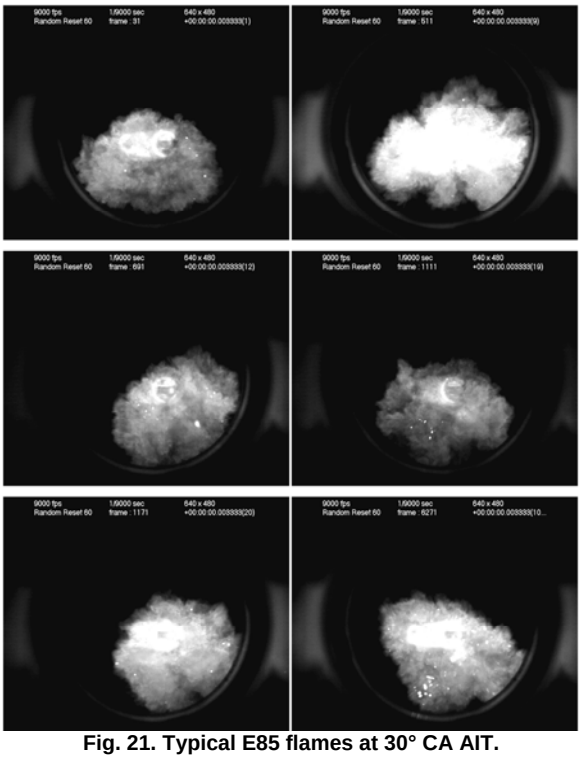

Fig. 21. Typical E85 flames at 30° CA AIT.

The use of flame imaging is advantageous in many ways over straight pressure data because it allows physical changes in flame shape and motion to be directly visualised on a cycle by cycle basis and correlated to pressure-related parameters to try to identify potentially desirable features of flame propagation. This is particularly relevant for analysis of cyclic variability where early flame growth features have been shown to affect the final 'quality' of a cycle [16]. Flame imaging can also reveal information about the surrounding flow field as it interacts with the flame or potential temperature and concentration gradients as 'seen' by the flame which are reflected in spatial and image intensity variations. The results show that the E85 flames grow in similar shapes and sizes to gasoline flames but there are differences in the intensities and textures of the flames of these two fuels. The flames of E85 were distinctively 'foggy' in appearance without the level of detail within the flame exhibited by gasoline flames. This result has also been observed with a variety of pure alcohols using the same engine, but different injector geometry [11] and will be studied further by laser-sheet flame tomography. E85 also shows smaller bright spots compared to gasoline which may relate to lower soot production.

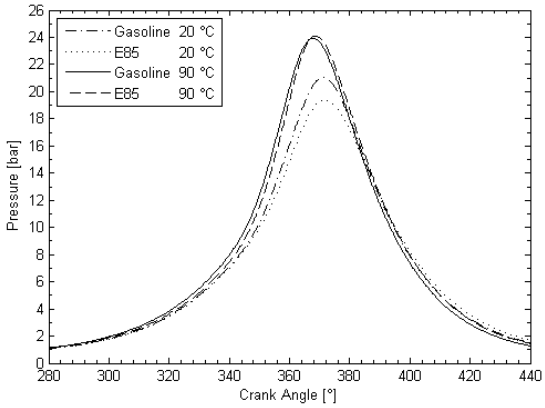

Fig. 22. Average in-cylinder pressure for gasoline and E85 (ignition timing fixed at 325 °CA).

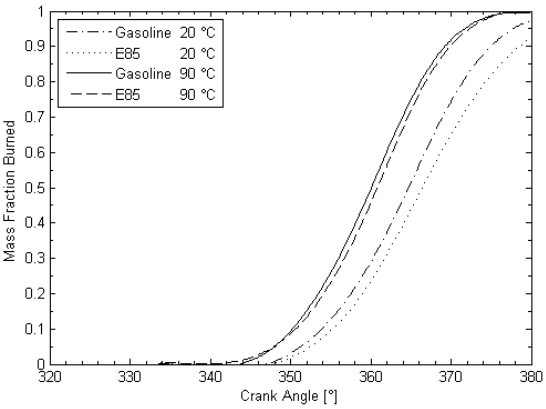

Fig. 23. Average mass fraction burned for gasoline and E85 (ignition timing fixed at 325 °CA).

Combustion performance was very similar for gasoline and E85 at hot engine conditions as shown by the average in-cylinder pressure traces and mass fraction burned curves in Figure 22 and 23, respectively, although there is potentially some room for ignition timing optimisation at 20 °C. Slower combustion

development for E85, especially at cold engine conditions indicated possibly the effect of increased charge cooling and the necessity of advancing ignition timing to match gasoline performance. A recent study of in-cylinder pressures and mass fraction burned traces with direct injection of gasoline and E85 using a multi-hole injector has shown higher peak pressures and faster burning rates with E85 in comparison to gasoline at optimised ignition timings for the two fuels [17].

6. Conclusions and Future Work

The study presented in this paper compared the spray properties of E85 with gasoline RON95 using high-speed imaging techniques and PDA to obtain high-resolution spray development data and droplet sizes. Results were presented for an optical quiescent pressure chamber and an optical DISI engine. The results showed that on average E85 and gasoline sprays exhibited similar macroscopic characteristics. However, there were some specific differences; those key findings are summarised below:

- E85 had visibly thinner and more compact plumes than gasoline at 20 °C, leading to higher spray tip penetration at 0.5 bar and 1.0 bar gas pressures in the quiescent chamber. The observations also hold in the engine but flow-field effects were found to disguise some of the differences due to higher levels of break-up resulting from spray/flow interactions.

- E85 showed smaller sensitivity to fuel temperature than gasoline and as a result experienced spray collapse to a lesser extent at 120 °C in the pressure chamber. Similar trends and levels of collapse were observed in the engine at 90 °C.

- Spray tip penetrations measured in the quiescent chamber were always higher for E85 by 5–10% compared to gasoline, except at the 0.5 bar gas pressure and 120 °C condition, where gasoline's penetration was higher due to the heavily collapsed spray producing a greater momentum in the vertical component of motion.

- Overall spray cone angles for E85 were similar or slightly larger than gasoline at comparable quiescent conditions. The overall spray cone angles at 20 °C were both ~59° but the lower propensity of E85 sprays to collapse was demonstrated as a higher cone angle at 120 °C by ~8%, at 52° compared to 48° for gasoline.

- Droplet sizes at 25 mm below the injector tip were found to be larger for E85 by 22–33%, with the biggest differences calculated occurring at 0.5 bar gas pressure and 20 °C. This effect was also noticeable in the engine from RMS spray images which showed the presence of large droplets below the spray in contrast to gasoline where no such droplets were imaged.

- Combustion development in terms of mass fraction burned was found to be slightly slower for E85 at low coolant temperatures but only marginally slower at high coolant temperatures. It is expected that small adjustments in ignition timing would improve the performance of E85 to similar level of gasoline, although the poorer atomisation for E85 is likely to be a contributor to the lower performance seen at 20 °C.

Further work is needed to understand the differences in spray development between the two fuels, including analysis of the regimes of atomisation with respect to Weber and Ohnesorge numbers, as well as studies of in-nozzle flash boiling at high-temperature and low-pressure conditions. It is also needed to quantify the differences between the two fuels with respect to flame growth speeds and directions of in-cylinder motion by post-processing the acquired flame images. The latter study will be complemented by laser-sheet flame imaging to identify structural differences in the flame front for the two fuels.

References

[1] Fachetti, A. and Kremer, F.G., "Alcohol as an Automotive Fuel – Updated Vision of the Brazilian Experience", FISITA 2004, Paper F2004V175, 2004.

[2] Larive, J.F., "Well-to-Wheel Analysis – A Necessary Evil when Evaluating Biofuel Options", International Biofuels Opportunities, Royal Society, London, 2007.

[3] Wang, W., "Well-to-Wheel Analysis of Transportation Fuels with GREET Model", Advanced Stationary Reciprocating Engines Conference, Downey, CA, September 19th, 2007.

[4] Porter, J.C., "Alcohol as a High Octane Fuel", SAE Paper 510086.

[5] Gautam, M. and Martin, D.W., "Combustion Characteristics of Higher Alcohol/Gasoline Blends", Proceedings of IMechE, Part A, Vol. 214, pp.497–511, 2000.

[6] Nakata, K., Utsumi, S., Ota, A., Kawate, K., Kawai, T. and Tsunooka, T., "The Effect of Ethanol on a Spark Ignition Engine", SAE Paper 2006-01-3380, 2006.

[7] Aleiferis, P.G., Malcolm, J.S., Todd, A.R., Cairns, A. and Hoffman, H., "An Optical Study of Spray Development and Combustion of Ethanol, Iso-Octane and Gasoline in a DISI Engine", SAE Paper 2008-01-0073, 2008.

[8] van Romunde, Z., Aleiferis, P.G., Cracknell, R.F. and Walmsley, H.L., "Effect of Fuel Properties on Spray Development from a Multi-Hole DISI Engine Injector", SAE Transactions, Journal of Engines, Vol. 116, pp. 1313–1331, SAE Paper 2007-01-4032, 2007.

[9] Serras-Pereira, J., Aleiferis, P.G., Richardson, D. and Wallace, S., "Mixture Preparation and Combustion Variability in a Spray-Guided DISI engine", SAE Transactions, Journal of Engines, Vol. 116, pp. 1332–1356, SAE Paper 2007-01-4033, 2007.

[10] van Romunde, Z. and Aleiferis, P.G., "Effect of Operating Conditions and Fuel Volatility on Development and Variability of Sprays from Gasoline Direct-Injection Multi-Hole Injectors",

Atomization and Sprays, Vol. 19, pp. 207–234, 2009.

[11] Serras-Pereira, J., Aleiferis, P.G., Richardson, D. and Wallace, S., “Characteristics of Ethanol, Butanol, Iso-Octane and Gasoline Sprays and Combustion from a Multi-Hole Injector in a DISI Engine”, SAE Transactions, Journal of Fuels and Lubricants, Vol. 117, SAE Paper 2008-01-1591, 2008.

[12] Mitroglou, N., Nouri, J.M., Yan, Y., Gavaises, M. and Arcoumanis, C., “Spray Structure Generated by Multi-Hole Injectors for Gasoline Direct-injection Engines”, SAE Paper 2007-01-1417, 2007.

[13] Mariott, C.D., Wiles, M., Gwidt, J.M. and Parrish, S.E., “Development of a Naturally Aspirated Spark Ignition Direct Injected Flex-Fuel Engine”, SAE Paper 2008-01-0319, 2008.

[14] Gao, J., Jiang, D. and Huang, Z., “Spray Properties of Alternative Fuels: A Comparative Analysis of Ethanol-Gasoline Blends and Gasoline”, Fuel, Vol. 86, pp. 1645–1650, 2007.

[15] Taniguchi, S., Yoshida, K. and Tsukasaki, Y., “Feasibility Study of Ethanol Applications to a Direct-Injection Gasoline Engine”, SAE Paper 2007-01-2037, 2007.

[16] Aleiferis, P.G., Taylor, A.M.K.P., Ishii, K. and Urata, Y., “The Nature of Early Flame Development in a Lean-Burn Stratified-Charge Spark-Ignition Engine”, Combustion and Flame, Vol. 136, pp. 283–302, 2004.

[17] Zhu, G., Stuecken, T., Schock, H. and Yang, X., Hung, D.L.S. and Fedewa, A., “Combustion Characteristics of a Single-Cylinder Engine Equipped with Gasoline and Ethanol Dual-Fuel Systems”, SAE Paper 2008-01-1767, 2008.